Quantum Interference in the fluorescence of a molecular system

Author

Wang, J, Wiseman, HM, Ficek, Z

Published

2000

Journal Title

Physical Review A: Atomic, Molecular and Optical Physics

DOI

10.1103/PhysRevA.62.013818

Quantum interference in the fluorescence of a molecular system

Jin Wang[1,2], H.M. Wiseman[1,2], and Z. Ficek[1,3]
[1] *Centre for Laser Science and Department of Physics, The University of Queensland, Brisbane, Queensland 4072, Australia*
[2] *School of Science, Griffith University, Nathan, Brisbane, Queensland 4111, Australia*
[3] *Department of Applied Mathematics and Theoretical Physics, The Queen's University of Belfast, Belfast BT7 1NN, Northern Ireland*
(February 1, 2008)

It has been observed experimentally [H.R. Xia, C.Y. Ye, and S.Y. Zhu, Phys. Rev. Lett. **77**, 1032 (1996)] that quantum interference between two molecular transitions can lead to a suppression or enhancement of spontaneous emission. This is manifested in the fluorescent intensity as a function of the detuning of the driving field from the two-photon resonance condition. Here we present a theory which explains the observed variation of the number of peaks with the mutual polarization of the molecular transition dipole moments. Using master equation techniques we calculate analytically as well as numerically the steady-state fluorescence, and find that the number of peaks depends on the excitation process. If the molecule is driven to the upper levels by a two-photon process, the fluorescent intensity consists of two peaks regardless of the mutual polarization of the transition dipole moments. If the excitation process is composed of both a two-step one-photon process and a one-step, two-photon process, then there are two peaks on transitions with parallel dipole moments and three peaks on transitions with antiparallel dipole moments. This latter case is in excellent agreement with the experiment.

I. INTRODUCTION

There have been a large number of theoretical studies on the effects of quantum interference in atomic and molecular systems [1]. This phenomenon was first suggested by Agarwal [2] who showed that the spontaneous emission from a degenerate V-type three-level atom is sensitive to the mutual orientation of the atomic dipole moments. If they are parallel a suppression of spontaneous emission can appear and a part of the population can be trapped in the excited levels. Similar predictions were reported for other configurations of three- and multi-level atoms and show that quantum interference can lead to many interesting effects such as amplification without population inversion [3], electromagnetically-induced transparency [4], phase dependent spectra and population inversions [5], and ultranarrow spectral lines [6].

Zhu and Scully [7] and Lee *et al.* [8] have shown that in the case of a non-degenerate V-type atom driven from an auxiliary level, quantum interference can lead to the elimination of the central line in the fluorescence spectrum when the driving field is tuned to the middle of the upper levels splitting. This interesting effect suggests that quantum interference can be used as a mechanism for controlling and even for suppression of spontaneous emission.

In 1996, Xia *et al.* [9] carried out the first experimental investigation of constructive and destructive interference effects in spontaneous emission. In the experiment they used sodium dimers, which can be modeled as five-level molecular systems with a single ground level, two intermediate and two upper levels, driven by a two-photon process from the ground level to the upper doublet. By monitoring the fluorescence from the upper levels they observed that the total fluorescent intensity, as a function of two-photon detuning, is composed of two peaks on transitions with parallel and three peaks on transitions with antiparallel dipole moments. The observed variation of the number of peaks with the mutual polarization of the dipole moments gives compelling evidence for quantum interference in spontaneous emission.

It is our purpose in this paper to present a theoretical explanation of the observed fluorescent intensity and, in particular, to explain the variation of the number of the observed peaks with the mutual polarization of the molecular dipole moments. We point out here that the previous theoretical studies [7,8] of quantum interference between two transitions with parallel or antiparallel dipole moments have dealt with the fluorescence *spectrum*. By contrast in the experiment, the *total* fluorescent intensity, as a function of two-photon detuning, was observed. Agarwal [10] has provided an intuitive picture for the observed spontaneous emission cancellation in terms of interference pathways involving a two-photon absorption process. Recently, Berman [11] has shown that the experimentally observed cancellation of spontaneous emission involving a two-photon absorption process can be interpreted in terms of population trapping. Although a cancellation of spontaneous emission is present with a two-photon excitation process, no variation of the number of peaks with the polarization of the dipole moments exist in the fluorescent intensity.

In summary, no explanation has been offered until now for the observed variation of the number of peaks in the fluorescent intensity with the mutual polarization of the transition dipole moments.

In this paper we consider a five-level system driven by a single-mode coherent laser field, which models the experimental configuration set up by Xia *et al.* [9]. Working with the master equation of the system, we calculate the steady-state fluorescent intensity as a function of the laser frequency for two different transitions from the upper levels to intermediate levels. One transition is in the visible region and has parallel dipole moments. The other transition is in the ultraviolet and has antiparallel dipole moments. We assume that there is spontaneous emission from the upper to the intermediate levels and thence to the ground level so the dynamics of the system are restricted to these five levels. In a real sodium molecule, the situation is more complex, with other decay channels, and laser-field couplings between various real states [12]. However, we believe that our simple model does explain the basic physical effects which have been observed in the experiment.

In Xia's paper [9] the excitation of the upper states is described as a two-photon process. As we will see later, the two photon excitation process can only ever lead to two peaks in the fluorescent intensity, independent of the mutual polarization of the dipole moments. We show that the experimentally observed variation of the number of peaks arises from the presence of an additional two-step, one-photon excitation processes.

The paper is organized as follows. The master equation for the five-level molecular system driven by a single mode laser field is derived and analyzed in section II. The analytical and numerical results for the total fluorescent intensity for the two-photon coupling only are studied in section III. In section IV, we investigate the corresponding results when the system has both one- and two-photon coupling. We also examine the approximations made and make comparisons with the experimental results. A discussion is given in the concluding section V.

II. THE MASTER EQUATION

The energy-level scheme of the system we are considering is shown in Fig. 1, in which we follow the notation of Ref. [9]. The five-level molecule consists of two upper levels $|a_1\rangle$ and $|a_2\rangle$, two intermediate levels $|b\rangle$ and $|d\rangle$, and a single ground level $|c\rangle$. The upper levels are separated by the frequency ω_{12} which is much smaller than the frequencies ω_{1b} and ω_{2b} of the $|a_1\rangle \to |b\rangle$ and $|a_2\rangle \to |b\rangle$ transitions and the frequencies ω_{1d} and ω_{2d} of the $|a_1\rangle \to |d\rangle$ and $|a_2\rangle \to |d\rangle$ transitions. As in the sodium dimers used in the Xia's experiment [9], we assume that the frequencies ω_{1b} and ω_{2b} are significantly different from the frequencies ω_{1d} and ω_{2d}. The transitions $|a_1\rangle, |a_2\rangle \to |b\rangle$ correspond to the visible region, whereas the transitions $|a_1\rangle, |a_2\rangle \to |d\rangle$ correspond to the uv region.

In the molecule, the one-photon transitions $|a_1\rangle, |a_2\rangle \to |b\rangle, |d\rangle \to |c\rangle$ are connected by electric dipole moments, whereas the transition $|a_1\rangle \to |a_2\rangle$ and the two-photon transitions $|a_1\rangle, |a_2\rangle \to |c\rangle$ are forbidden in the electric dipole approximation. The molecular dipole moments can have different orientations (polarizations) and two dipole moments which are close in frequency can interfere with each other if they are not orthogonal. In the experiment, a destructive interference was observed between two transitions, $|a_1\rangle \to |b\rangle$ and $|a_2\rangle \to |b\rangle$, with parallel dipole moments, and a constructive interference was observed between transitions $|a_1\rangle \to |d\rangle$ and $|a_2\rangle \to |d\rangle$ with antiparallel dipole moments.

In order to quantify the mutual orientations of the transition dipole moments, we introduce a parameter

$$p = \frac{\vec{\mu}_{ij} \cdot \vec{\mu}_{kl}}{|\vec{\mu}_{ij}||\vec{\mu}_{kl}|}, \qquad ij \neq kl, \tag{2.1}$$

where $\vec{\mu}_{ij}$ is the matrix element of the transition dipole moment between $|i\rangle$ and $|j\rangle$ levels. Using the subscripts u and v to denote the ultraviolet and visible transitions in the experiment, we have $p_u = 1$ (parallel dipole moments), while $p_v = -1$ (antiparallel dipole moments).

For simplicity we will assume that the magnitude of the interfering dipole moments are the same. Thus, the upper doublet decays to level $|b\rangle$ at rate $\gamma_v = \gamma_{1b} = \gamma_{2b}$ and to level $|d\rangle$ at rate $\gamma_u = \gamma_{1d} = \gamma_{2d}$. Here u and v again refer to visible and ultraviolet. The intermediate levels $|b\rangle$ and $|d\rangle$ decay to the ground level $|c\rangle$ at rates γ_b and γ_d respectively.

The system is driven by a single-mode tunable laser of frequency ω_L. In the experiment the dye laser was coupled to the two-photon transition $|c\rangle \to |a_1\rangle, |a_2\rangle$ in order to avoid the Doppler effect (which we ignore in our analysis). Here, we must ask a question whether the two-photon coupling in the experiment was the only coupling of the laser to the system. It is stated in the experimental paper [9] that the two-photon transition in sodium dimers was enhanced by a near-resonant intermediate level, indicating that the laser could also couple the ground state $|c\rangle$ to the upper states $|a_1\rangle, |a_2\rangle$ via cascaded one-photon transitions. Here, to avoid introducing an extra level, we take the near-resonant intermediate level to be $|b\rangle$, so the laser can also produce a two-step one-photon transition $|c\rangle \to |b\rangle$ then $|b\rangle \to |a_1\rangle, |a_2\rangle$. In our opinion this channel of the excitation was possible in the experiment as the one-photon transitions in the molecule are in the visible region and their dipole moments are parallel [9]. We will see later that the presence of this channel of excitation will be crucial in the explanation of the experimentally observed fluorescent

intensity profile. With only two-photon excitation quantum interference can be observed but the fluorescent intensity exhibits two peaks (as a function of laser detuning) regardless of the mutual orientation of the transition dipole moments. The three peak structure of the fluorescent intensity observed in the experiment in the uv region can only result from the presence of the two-step one-photon channel.

We calculate the steady-state intensity of the fluorescence from the upper doublet to the intermediate levels as follows. The intensity is proportional to the normally ordered first-order correlation function of the scattered field

$$I\left(\vec{r},t\right) \propto \left\langle \vec{E}^{(-)}\left(\vec{r},t\right)\cdot\vec{E}^{(+)}\left(\vec{r},t\right)\right\rangle, \tag{2.2}$$

where $\vec{E}^{(+)}\left(\vec{r},t\right)$ is the positive frequency part of the electric field operator at a point $\vec{r}$ in the far-field zone of the system outside the driving laser field. In terms of the density matrix elements of the system the scaled steady-state ($t\rightarrow\infty$) intensity on the ultraviolet and visible transitions is

$$I_{u/v} = \gamma_{u/v}\left(\rho_{11}+\rho_{22}+2p_{u/v}\mathrm{Re}\rho_{12}\right). \tag{2.3}$$

Here ρ_{11} and ρ_{22} are the steady-state populations of the level $|a_1\rangle$ and $|a_2\rangle$, and ρ_{12} is the stead-state coherence between them.

We find steady-state values of the populations and coherences from the master equation of the system. The master equation can be written in the Lindblad form [13] as

$$\dot{\rho} = \mathcal{L}_{\mathrm{rev}}\rho + \mathcal{L}_{\mathrm{irr}}\rho, \tag{2.4}$$

where the reversible and irreversible terms are, respectively

$$\mathcal{L}_{\mathrm{rev}}\rho = -i[H,\rho], \tag{2.5}$$

and

$$\begin{aligned}\mathcal{L}_{\mathrm{irr}} &= \gamma_v\left(1+p_v\right)\mathcal{D}\left[|b\rangle(\langle a_1|+\langle a_2|)/\sqrt{2}\right]+\gamma_v\left(1-p_v\right)\mathcal{D}\left[|b\rangle(\langle a_1|-\langle a_2|)/\sqrt{2}\right]\\ &\quad+\gamma_u\left(1+p_u\right)\mathcal{D}\left[|d\rangle(\langle a_1|+\langle a_2|)/\sqrt{2}\right]+\gamma_u\left(1-p_u\right)\mathcal{D}\left[|d\rangle(\langle a_1|-\langle a_2|)/\sqrt{2}\right]\\ &\quad+\gamma_b\mathcal{D}[|c\rangle\langle b|]+\gamma_d\mathcal{D}[|c\rangle\langle d|] \qquad (2.6)\\ &= \gamma_v\mathcal{D}\left[|b\rangle(\langle a_1|-\langle a_2|)\right]+\gamma_u\mathcal{D}\left[|b\rangle(\langle a_1|+\langle a_2|)\right]+\gamma_b\mathcal{D}[|c\rangle\langle b|]+\gamma_d\mathcal{D}[|c\rangle\langle d|]. \qquad (2.7)\end{aligned}$$

Here, $\mathcal{D}$ is a superoperator defined for arbitrary operators A and B as

$$\mathcal{D}[A]B \equiv ABA^{\dagger}-\tfrac{1}{2}\{A^{\dagger}A,B\}. \tag{2.8}$$

Taking the ground state to have zero energy, the Hamiltonian operator in Eq. (2.5) (working in units where $\hbar=1$) can be split as $H=H_0+H_1$, where

$$H_0 = 2\omega_L|a_1\rangle\langle a_1|+2\omega_L|a_2\rangle\langle a_2|+\omega_L|b\rangle\langle b|+\omega_d|d\rangle\langle d| \tag{2.9}$$

is approximately equal to the Hamiltonian of the molecular system, and

$$\begin{aligned}H_1 &= \left[\Omega_{bc}|b\rangle\langle c|e^{-i\omega_L t}+\mathrm{H.c.}\right]+\left[\Omega_{ab}\left(|a_1\rangle+|a_2\rangle\right)\langle b|e^{-i\omega_L t}+\mathrm{H.c.}\right]\\ &\quad+\left[Q\left(|a_1\rangle+|a_2\rangle\right)\langle c|e^{-i2\omega_L t}+\mathrm{H.c.}\right]\\ &\quad+(\omega_1-2\omega_L)|a_1\rangle\langle a_1|+(\omega_2-2\omega_L)|a_2\rangle\langle a_2|+(\omega_b-\omega_L)|b\rangle\langle b|+(\omega_d-\omega_L)|d\rangle\langle d|\end{aligned} \tag{2.10}$$

includes the interaction with the laser field plus corrections to H_0 to reproduce the full molecular Hamiltonian.

The first and second terms in Eq. (2.10) describe the interaction of the classical laser field with electric dipole moments of the one-photon transitions $|c\rangle\rightarrow|b\rangle$ and $|b\rangle\rightarrow|a_1\rangle,|a_2\rangle$, respectively. The strengths with which these transitions are driven are characterized by the one-photon Rabi frequencies $\Omega_{bc}=\frac{1}{2}\vec{\mu}_{bc}\cdot\vec{E}_L$, and $\Omega_{ab}=\frac{1}{2}\vec{\mu}_{ba_1}\cdot\vec{E}_L=\frac{1}{2}\vec{\mu}_{ba_2}\cdot\vec{E}_L$, where $\vec{E}_L$ is the amplitude of the laser field.

The third term in Eq. (2.10) describes the two-photon coupling of the laser field to the system with the two-photon Rabi frequency

$$Q=\sum_m\frac{1}{2}\frac{\mu_{mc}\mu_{ma_1}E_L^2}{\omega_L-\omega_{mc}}=\sum_m\frac{1}{2}\frac{\mu_{mc}\mu_{ma_2}E_L^2}{\omega_L-\omega_{mc}}, \tag{2.11}$$

where $E_L = |\vec{E}_L|$. This is due to transitions via the intermediate virtual levels labelled m here.

Because of the external driving the elements of the system state matrix ρ satisfy equations of motion containing explicit time-dependent factors of the complex exponential type. These can be removed by moving to the interaction picture with respect to H_0. The remaining Hamiltonian H_1 becomes

$$\begin{aligned} H_I(t) = &(\omega_{12}/2 - \Delta)|a_1\rangle\langle a_1| \\ &+(-\omega_{12}/2 - \Delta)|a_2\rangle\langle a_2| \\ &+(-\Delta/2 - \delta)|b\rangle\langle b| \\ &+ [\Omega_{ab}\left(|a_1\rangle + |a_2\rangle\right)\langle b| + \text{H.c.}] \\ &+ [Q\left(|a_1\rangle + |a_2\rangle\right)\langle c| + \text{H.c.}] \\ &+ [\Omega_{bc}|b\rangle\langle c| + \text{H.c.}]\,. \end{aligned} \tag{2.12}$$

Although this is written as $H_I(t)$ it is actually time-independent because of the judicious choice of H_0. Here $\Delta = 2\omega_L - \omega_a$ is the detuning between the two-photon laser frequency $2\omega_L$ and the mean frequency of the upper levels relative to the ground level $\omega_a = (\omega_1 + \omega_2)/2$. The one-photon detuning $\delta = \omega_L - \Delta/2 - \omega_b = \omega_a/2 - \omega_b$ is the gap between the energy of level $|b\rangle$ and the half way position from the ground level $|c\rangle$ to the mean of the upper levels $|a_1\rangle$ and $|a_2\rangle$. Moving to the interaction picture does not affect the irreversible terms so the new master equation is

$$\dot{\rho} = \mathcal{L}_{\text{irr}}\rho - i[H_I, \rho]. \tag{2.13}$$

The stationary solution satisfying $\dot{\rho} = 0$ can be found numerically and, in certain limits, analytically. We consider separately the case of two-photon coupling only, and one- and two-photon coupling.

III. TWO-PHOTON COUPLING ONLY

The case where the upper pair of levels is excited only by two-photon transitions via virtual intermediate levels is found by setting Ω_{ab} and Ω_{bc} in the interaction Hamilltonian (2.12) equal to zero. The two-photon driving parametrized by Q is the only sort of driving mentioned in the experimental paper [9].

1. Analytical Solution

We first consider an analytical solution. This is possible in the weak-field limit where Q is much smaller than the decay rates in the system. For the experimentally relevant mutual polarizations $p_v = 1$, $p_u = -1$, the equations of motion are greatly simplified if we make the assumption that $\gamma_u = \gamma_v$. That is, we assume that the decay rates of the upper levels on the ultraviolet and visible transitions are equal. We therefore define a new parameter $\gamma_a = \gamma_u = \gamma_v$.

Under these assumptions, it is easy to show that the master equation (2.13) leads to the following steady-state values of the upper level populations and coherences

$$\rho_{11} = \frac{Q^2}{(\Delta + \omega_{12}/2)^2 + \gamma_a^2}, \tag{3.1}$$

$$\rho_{22} = \frac{Q^2}{(\Delta - \omega_{12}/2)^2 + \gamma_a^2}, \tag{3.2}$$

$$\text{Re}\rho_{12} = \frac{Q^2[\Delta^2 - (\omega_{12}/2)^2 + \gamma_a^2]}{[(\Delta + \omega_{12}/2)^2 + \gamma_a^2][(\Delta - \omega_{12}/2)^2 + \gamma_a^2]}. \tag{3.3}$$

These are shown in Fig. 2(a) as a function of Δ.

This analysis predicts that the populations and coherence exhibit peaks at $\Delta = \pm\omega_{12}/2$, corresponding to the two-photon resonances of the laser field with the $|c\rangle \rightarrow |a_1\rangle$ and $|c\rangle \rightarrow |a_2\rangle$ transitions. In Fig. 2(b), we plot the fluorescent intensity as a function of Δ for the $p_v = 1$ and $p_u = -1$ transitions. It is seen that there are two peaks located at $\Delta = \pm\frac{1}{2}\omega_{12}$, the amplitudes of which are not sensitive to p. The intensity is sensitive to p only about $\Delta = 0$ and can be almost completely suppressed for $p_v = 1$ transitions. This confirms the earlier prediction by Agarwal [10] that the two-photon excitation process involving the $|a_1\rangle$ and $|a_2\rangle$ levels can lead to cancellation of spontaneous emission to the level $|b\rangle$. The cancellation of the fluorescence at $\Delta = 0$ also confirms the prediction by Berman [11] that the suppression of the fluorescence can be explained in terms of dark states and coherent population trapping.

For $p_v = 1$ the fluorescent intensity (2.3) can be written as

$$I_v = 2\gamma_v \rho_{ss}, \tag{3.4}$$

where $\rho_{ss} = \langle s|\rho|s\rangle$ is the population of the symmetric $|s\rangle = (|a_1\rangle + |a_2\rangle)/\sqrt{2}$ combination of the upper levels. The suppression of the fluorescence at $\Delta = 0$ indicates that the state $|s\rangle$ is almost unpopulated in the steady-state. This implies that the population is trapped between other molecular levels, including the antisymmetric state $|a\rangle = (|a_1\rangle - |a_2\rangle)/\sqrt{2}$, with the state $|s\rangle$ being a dark state of the system.

A. Numerical Results

As noted before, in the experiment [9] three peaks were observed on the transitions with antiparallel dipole moments. However, as it is seen from Fig. 2(b), the weak-field theory does not predict three peaks for the $p_u = -1$ transitions. The reason is that the magnitude of the coherence term ρ_{12} is small compared to the magnitude of the population terms so that it is unable to build up a third peak in the middle. The coherence term is necessarily small because there is no detuning Δ at which both populations are large, and the coherence term is limited in magnitude by

$$|\rho_{12}|^2 \leq \rho_{11}\rho_{22}. \tag{3.5}$$

To prove that the lack of a third peak is not a result of the assumptions made in deriving the analytical results we have also studied numerically the steady state of the master equation (2.13) with the one-photon Rabi frequencies set to zero. This can be done by calculating the equations of motion for the density matrix elements and using matrix inversion techniques. It can be done more easily using the direct symbolic representation of the master equation (2.13) which is possible in the quantum optics toolbox for matlab [14]. We find that, even in the strong field limit, and even with $\gamma_u \neq \gamma_v$, it is not possible to produce a third peak in the fluorescence profile.

From these analytical and numerical results we conclude that as well as the two-photon excitation process there must be some other processes involved in the dynamics of the system. The obvious candidate is a two-step one-photon process.

IV. ONE- AND TWO-PHOTON COUPLING

To include one-photon coupling we now consider the case where Ω_{bc} and Ω_{ab} are nonzero. To include two-photon coupling we actually do not need to have Q nonzero. That is because, as we will show, there is a regime in which level $|b\rangle$ acts as a virtual level with almost no real population. In this limit, the two step one-photon process becomes equivalent to a two-photon process. The relative strength of the two- and one-photon couplings is given by a parameter $\alpha = \gamma_b/\gamma_a$, to be discussed later. Thus, for simplicity, we set $Q = 0$.

A. Analytical Results

To obtain analytical results we must consider the equations of motion for the density matrix elements. The master equation (2.13), in general, leads to a system of twenty five equations of motion for the density matrix elements. Because of the assumption of large non-degeneracy between the intermediate levels $|b\rangle$ and $|d\rangle$, the coherences $\rho_{cd}, \rho_{da_1}, \rho_{bd}$ and ρ_{da_2} are not coupled to the driving field, and then the system of equations splits into two subsystems: one of seventeen equations of motion directly coupled to the driving field and the other of eight equations of motion not coupled to the driving field. It is not difficult to show that the steady-state solutions for the eight density matrix elements are zero and therefore we limit our considerations to the seventeen equations which, after applying the trace property ($\mathrm{Tr}\rho = 1$), reduce to a system of sixteen coupled linear inhomogeneous equations.

As in the case of Sec. III 1, for the physical parameters $p_v = 1$, $p_u = -1$, the equations are simplified if $\gamma_u = \gamma_v$. Under this assumption, and substituting γ_a for both γ_u and γ_v, the relevant density matrix elements obey the following coupled equations

$$\dot{\rho}_{11} = -2\gamma_a\rho_{11} - i\Omega_{ab}\left(\rho_{b1} - \rho_{1b}\right), \tag{4.1}$$

$$\dot{\rho}_{22} = -2\gamma_a\rho_{22} - i\Omega_{ab}\left(\rho_{b2} - \rho_{2b}\right), \tag{4.2}$$

$$\dot{\rho}_{bb} = -\gamma_b\rho_{bb} + \gamma_a\left(\rho_{11} + \rho_{22} + \rho_{12} + \rho_{21}\right)$$

$$- i\Omega_{bc}\left(\rho_{cb}-\rho_{bc}\right)+i\Omega_{ab}\left(\rho_{b1}-\rho_{1b}\right)+i\Omega_{ab}\left(\rho_{b2}-\rho_{2b}\right), \tag{4.3}$$

$$\dot{\rho}_{cc}=\gamma_b\rho_{bb}+\gamma_d(1-\rho_{11}-\rho_{22}-\rho_{bb}-\rho_{cc})+i\Omega_{bc}\left(\rho_{cb}-\rho_{bc}\right), \tag{4.4}$$

$$\dot{\rho}_{12}=-\left(2\gamma_a+i\omega_{12}\right)\rho_{12}-i\Omega_{ab}\rho_{b2}+i\Omega_{ab}\rho_{1b}, \tag{4.5}$$

$$\dot{\rho}_{b2}=-\left[\left(\gamma_a+\gamma_b/2\right)-i\left(\delta-\Delta/2-\omega_{12}/2\right)\right]\rho_{b2}-i\Omega_{bc}\rho_{c2}-i\Omega_{ab}\rho_{12}+i\Omega_{ab}\rho_{bb}-i\Omega_{ab}\rho_{22}, \tag{4.6}$$

$$\dot{\rho}_{b1}=-\left[\left(\gamma_a+\gamma_b/2\right)-i\left(\delta-\Delta/2+\omega_{12}/2\right)\right]\rho_{b1}-i\Omega_{bc}\rho_{c1}-i\Omega_{ab}\rho_{12}+i\Omega_{ab}\rho_{bb}-i\Omega_{ab}\rho_{11}, \tag{4.7}$$

$$\dot{\rho}_{bc}=-\left[\gamma_b/2-i(\delta+\Delta/2)\right]\rho_{bc}-i\Omega_{bc}\left(\rho_{cc}-\rho_{bb}\right)-i\Omega_{ab}\left(\rho_{1c}+\rho_{2c}\right), \tag{4.8}$$

$$\dot{\rho}_{1c}=\left[-i(\omega_{12}/2-\Delta)-\gamma_a\right]\rho_{1c}-i\Omega_{ab}\rho_{bc}-\gamma_a\rho_{1c}+i\Omega_{bc}\rho_{1b}, \tag{4.9}$$

$$\dot{\rho}_{2c}=\left[i(\omega_{12}/2+\Delta)-\gamma_a\right]\rho_{2c}+i\Omega_{ab}\rho_{bc}-\gamma_a\rho_{2c}-i\Omega_{bc}\rho_{1b}. \tag{4.10}$$

To proceed further we make the weak-field assumption that Ω_{ab} and Ω_{bc} are small compared with the decay rates. We will show later that the same qualitative results can be obtained when this assumption, and the assumption $\gamma_u=\gamma_v$, are relaxed.

Under the weak field assumption we can order the matrix elements by how they scale with $\Omega\sim\Omega_{bc},\Omega_{ab}$ as shown in Fig. 3. The simplifications result from keeping only the lowest order terms in the above equations of motion for the state matrix elements. The steady-state solutions can then be obtained by setting the time derivatives to zero and solving the equations in the order as shown in Fig. 3. We find that the upper level populations are given by

$$\rho_{11}=\frac{\Omega_{ab}^2\Omega_{bc}^2}{[(\Delta/2+\delta)^2+\gamma_b^2/4][(\Delta-\omega_{12}/2)^2+\gamma_a^2]}, \tag{4.11}$$

$$\rho_{22}=\frac{\Omega_{ab}^2\Omega_{bc}^2}{[(\Delta/2+\delta)^2+\gamma_b^2/4][(\Delta+\omega_{12}/2)^2+\gamma_a^2]}. \tag{4.12}$$

This result predicts that, for large enough level splitting ω_{12}, the population of both of the upper pair states have two distinct peaks as a function of laser detuning Δ. This is illustrated in Fig. 4(a). The first peak is centered at $\Delta=\pm\omega_{12}/2$ for ρ_{11} or ρ_{22} respectively. At this detuning the two-photon transition from $|c\rangle$ to $|a_1\rangle$ or $|a_2\rangle$ is resonant, explaining the peak. The second peak is at $\Delta=-2\delta$. This is the resonance condition for the transition from $|c\rangle$ to $|b\rangle$, as seen in Fig. 1. This central peak results from two stepwise one-photon transitions, the first populating level $|b\rangle$ and the second exciting from $|b\rangle$ to $|a\rangle$. The populating of level $|b\rangle$ at this laser frequency is evident from the steady-state result

$$\rho_{bb}=\frac{\Omega_{ab}\Omega_{bc}}{[(\Delta/2+\delta)^2+\gamma_b^2/4]}. \tag{4.13}$$

The upper-states coherence is considerably more complicated, and is given in full in the Appendix. From the denominators in the expression given there, it is evident that ρ_{12} may have many peaks and this is also illustrated in Fig. 4(a). To discover the physical meaning out of such a complicated expression, we consider the limit of large splitting where ω_{12} is much larger than all other rates or frequencies. We then consider the behavior of ρ_{12} at the positions of its peaks, and keep only the leading contributions there. It turns out that only one peak survives this simplification:

$$\mathrm{Re}\rho_{12}\simeq\frac{-\Omega_{ab}^2\Omega_{bc}^2}{(\omega_{12}/2)^2\left[(\Delta/2+\delta)^2+(\gamma_b/2)^2\right]}. \tag{4.14}$$

From this expression it is evident that the coherence ρ_{12} also exhibits the resonance at $\Delta=-2\delta$, and its magnitude is comparable to the magnitude of population terms. This is possible because the populations ρ_{11} and ρ_{22} both have peaks at $\Delta=-2\delta$, resulting from two-step one-photon transitions. Thus the inequality in Eq. (3.5) allows the coherence (4.14) to have a peak here also, unlike the case with only two-photon transitions.

Assuming again that $\omega_{12}\gg\gamma_a,\gamma_b,\delta$, the peaks in the populations (4.11) and (4.12) are well-separated Lorentzians. Then using Eq. (4.14), the fluorescent intensity for the ultraviolet and visible transitions can be approximated as

$$I_{u/v}=\frac{16\gamma_{u/v}\Omega_{ab}^2\Omega_{bc}^2}{\omega_{12}^2}\left[\frac{1}{(\Delta-\omega_{12}/2)^2+\gamma_a^2}+\frac{1}{2}\frac{\left(1-p_{u/v}\right)}{(\delta+\Delta/2)^2+\left(\gamma_b/2\right)^2}+\frac{1}{(\Delta+\omega_{12}/2)^2+\gamma_a^2}\right]. \tag{4.15}$$

In this limit the fluorescent intensity contains three Lorentzians located at $\Delta=\pm\omega_{12}/2$ and $\Delta=-2\delta$. This is seen in the complete analytical solution for the fluorescence, from Eqs. (4.11), (4.12), and (5.1), plotted in Fig. 4(b). The amplitude of the peak at $\Delta=-2\delta$ strongly depends on the mutual polarization of the dipole moments. The peak

is absent in the intensity I_v observed in the visible region with $p_v = 1$. For the fluorescent intensity I_u observed in the uv region with $p_u = -1$, the amplitude of the peak is enhanced. The strong dependence of the amplitude of the central peak on the mutual orientation of the molecular dipole moments is precisely the effect observed in the experiment. We emphasize again that the presence of the central peak in the fluorescent intensity results from the coupling of the driving laser to the one-photon transitions.

B. Numerical results

Having illustrated the role of the one- and two-photon excitations in the weak-field limit, we now find the fluorescent intensity without making any simplifying assumptions in our model. In this case it is not possible to obtain analytical solutions and therefore we use numerical methods to find stationary values of the density matrix elements of the system. Once again, this is easy using the symbolic representational power of the quantum optics toolbox for matlab [14]. We first verify the correctness of the numerical technique by reproducing the weak-field analytical results. This is shown in Fig. 4(c).

In Fig. 5, we plot the fluorescent intensity for a strong driving field. It is seen that the fluorescent intensity exhibits the same behavior as that for the weak driving field, shown in Fig. 4, despite the fact that the solutions have been derived in different regimes.

The experimentally observed fluorescent intensity was asymmetric about $\Delta = 0$. There are few factors which could contribute towards the observed asymmetry. For example, the decay rates from the two upper levels to the intermediate levels could be unequal. A simpler reason could be that the central peak is not exactly at $\Delta = 0$. The analytical solution (2.3) predicts the central peak to be at $\Delta = -2\delta$ and the condition of $\delta = 0$ implies that the energy of the level $|b\rangle$ is exactly half of the mean energy of the upper levels. There is no reason to expect this condition to be satisfied in the real molecule, and in fact it appears from the experimental results that δ is positive. Fig. 7 shows the effect of a non-zero δ on the fluorescence profile for a strong driving field.

The relative magnitude of the central peak to the magnitude of the side peaks at $\Delta = \pm\omega_{12}/2$ depends on the ratio $\alpha = \gamma_b/\gamma_a$. In Fig. 6 we show the effect of α on the amplitude of the central peak in the fluorescent intensity on the uv transition. It is seen that the relative amplitude of the central peak increases with decreasing α (although the overall fluorescent intensity decreases). The exact size of the central peak compared to the side peaks depends on Ω and ω_{12} as well as α. A small value of α, which results in a large central peak as observed in the experiment, is consistent with the fact that the decay rates of the intermediate levels are much smaller than the decay rates of the upper levels [12]. When α increases the central peak becomes relatively smaller, and disappears completely for sufficiently large α. In this case the middle level is scarcely populated (because of its large decay rate) and the dynamics of the system are dominated by a two-photon process where the upper levels are directly populated from the ground level. Thus the large α limit is equivalent to considering only two-photon processes as in Sec. III, and it is not surprising that the spectrum contains only two peaks as found in that section.

Finally, in Fig. 8 we show numerically that the results are not much affected if we relax our previous assumption that γ_u and γ_v are equal (with their value being denoted by γ_a). For this plot we choose γ_u and γ_v to be different by more than a factor of two. The numerical results in this figure, and all of the above figures, indicate that the existence of the third peak is a robust feature which does not depend upon fine tuning of the parameters in the model.

V. SUMMARY

We have modeled quantum interference effects in the intensity of the fluorescence emitted from a five-level molecular system, studied experimentally by Xia *et al.* [9]. We have presented an analytical solution for the fluorescent intensity, valid in the weak-field limit, and a numerical solution valid for arbitrary strengths of the driving field. We have been particularly interested in a theoretical explanation of the experimentally observed dependence of the number of peaks in the fluorescent intensity on the mutual orientation of the transition dipole moments. We have assumed that the molecular excitation is composed of a one-step, two-photon absorption process, and a two-step process involving the absorption of a single photon in each step. If the excitation is composed of only the two-photon processes, the fluorescent intensity consists of two peaks regardless the mutual orientation of the molecular dipole moments. With the two-step, one-photon processes included, the intensity consists of two peaks on transitions with parallel dipole moments and three peaks on transitions with antiparallel dipole moments. This latter case is in excellent agreement with the experimental observation [9]. The variation of the number of peaks with the mutual polarization of the dipole moments is a very clear demonstration of quantum interference in spontaneous emission.

ACKNOWLEDGMENTS

This work has been supported by the Australian Research Council, the University of Queensland, Griffith University, and the Department of Employment, Education and Training, Australia. We appreciate valuable discussions with G.J. Milburn.

APPENDIX

The complete analytical solution to the upper level coherence in the weak driving limit with $\gamma_u = \gamma_v = \gamma_a$ is

$$
\begin{aligned}
\mathrm{Re}\rho_{12} = (\Omega_{ab}\Omega_{bc})^2 \big[&\gamma_b\gamma_a(\delta-\Delta/2+\omega_{12}/2)(\Delta-\omega_{12}/2)+\gamma_b{\gamma_a}^2(\gamma_a+\gamma_b)/2\\
&+2{\gamma_a}^2(\delta-\Delta/2+\omega_{12}/2)(\Delta/2+\delta)-\gamma_a(2\gamma_a+\gamma_b)(\Delta-\omega_{12}/2)(\Delta/2+\delta)/2\\
&+\omega_{12}(\delta-\Delta/2+\omega_{12}/2)(\Delta-\omega_{12}/2)(\Delta/2+\delta)+\omega_{12}\gamma_a(2\gamma_a+\gamma_b)(\Delta/2+\delta)/2\\
&-\omega_{12}\gamma_a\gamma_b(\delta-\Delta/2+\omega_{12}/2)/2+\omega_{12}\gamma_b(2\gamma_a+\gamma_b)(\Delta-\omega_{12}/2)/4]\\
&\div\big\{[(\delta-\Delta/2+\omega_{12}/2)^2+(2\gamma_a+\gamma_b)^2/4][(\Delta-\omega_{12}/2)^2+{\gamma_a}^2]\\
&[(\delta+\Delta/2)^2+\gamma_b^2/4][4{\gamma_a}^2+{\omega_{12}}^2]\big\}\\
&+(\Omega_{ab}\Omega_{bc})^2\big[\gamma_b\gamma_a(\delta-\Delta/2-\omega_{12}/2)(\Delta+\omega_{12}/2)/2+\gamma_b{\gamma_a}^2(2\gamma_a+\gamma_b)/2\\
&+2{\gamma_a}^2(\delta-\Delta/2-\omega_{12}/2)(\Delta/2+\delta)-\gamma_a(2\gamma_a+\gamma_b 2)(\Delta+\omega_{12}/2)(\Delta/2+\delta)/2\\
&+\omega_{12}(\delta-\Delta/2-\omega_{12}/2)(\Delta+\omega_{12}/2)(\Delta/2+\delta)+\omega_{12}(2\gamma_a+\gamma_b)\gamma_a(\Delta/2+\delta)/2\\
&-\omega_{12}\gamma_a\gamma_b(\delta-\Delta/2-\omega_{12}/2)/2+\omega_{12}\gamma_b(2\gamma_a+\gamma_b)(\Delta+\omega_{12}/2)/4]\\
&\div\big\{[(\delta-\Delta/2-\omega_{12}/2)^2+(2\gamma_a+\gamma_b)^2/4][(\Delta+\omega_{12}/2)^2+{\gamma_a}^2]\\
&[(\delta+\Delta/2)^2+\gamma_b^2/4][4{\gamma_a}^2+{\omega_{12}}^2]\big\}\\
&+\frac{\Omega_{ab}^2\Omega_{bc}^2[-\gamma_a(2\gamma_a+\gamma_b)-(\delta-\Delta/2+\omega_{12}/2)\omega_{12}]}{[(\delta-\Delta/2+\omega_{12}/2)^2+(2\gamma_a+\gamma_b)^2/4][(\delta+\Delta/2)^2+\gamma_b^2/4][4{\gamma_a}^2+{\omega_{12}}^2]}\\
&+\frac{\Omega_{ab}^2\Omega_{bc}^2[-\gamma_a(2\gamma_a+\gamma_b)-(\delta-\Delta/2-\omega_{12}/2)\omega_{12}]}{[(\delta-\Delta/2-\omega_{12}/2)^2+(2\gamma_a+\gamma_b)^2/4][(\delta+\Delta/2)^2+\gamma_b^2/4][4{\gamma_a}^2+{\omega_{12}}^2]}.
\end{aligned}
\tag{5.1}
$$

[1] E. Arimondo, in *Progress in Optics XXXV*, edited by E. Wolf (Elsevier, Amsterdam, 1996), p. 257.

[2] G.S. Agarwal, in *Quantum Statistical Theories of Spontaneous Emission and their Relation to Other Approaches*, edited by G. Hohler, Springer Tracts in Modern Physics, Vol. 70 (Springer, Berlin, 1974).

[3] S.E. Harris, Phys. Rev. Lett. **62**, 1033 (1989); M.O. Scully, S.-Y. Zhu and A. Gavrielides, Phys. Rev. Lett. **62**, 2813 (1989); G.S. Agarwal, Phys. Rev. A**44**, R28 (1991); C.H. Keitel, O. Kocharovskaya, L.M. Narducci, M.O. Scully, S.-Y. Zhu and H.M. Doss, Phys. Rev. A**48**, 3196 (1993); J. Kitching and L. Hollberg, Phys. Rev. A**59**, 4685 (1999).

[4] K.J. Boller, A. Imamoglu and S.E. Harris, Phys. Rev. Lett. **66**, 2593 (1991); K. Hakuta, L. Marmet and B. Stoicheff, Phys. Rev. Lett. **66**, 596 (1991); J.C. Petch, C.H. Keitel, P.L. Knight and J.P. Marangos, Phys. Rev. A**53**, 543 (1996).

[5] A.K. Patnaik and G.S. Agarwal, J. Mod. Opt. **45**, 2131 (1998); E. Paspalakis, C.H. Keitel and P.L. Knight, Phys. Rev. A**58**, 4868 (1998); S. Menon and G.S. Agarwal, Phys. Rev. A**57**, 4014 (1998); S.-Q. Gong, E. Paspalakis and P.L. Knight, J. Mod. Opt. **45**, 2433 (1998).

[6] P. Zhou and S. Swain, Phys. Rev. Lett. **77**, 3995 (1996); Phys. Rev. A**56**, 3011 (1997).

[7] S.-Y. Zhu and M.O. Scully, Phys. Rev. Lett. **76**, 388 (1996).

[8] H. Lee, P. Polynkin, M.O. Scully and S.Y. Zhu, Phys. Rev. A **55**, 4454 (1997); F.-L. Li and S.-Y. Zhu, Phys. Rev. A**59**, 2330 (1999).

[9] H.R. Xia, C.Y. Ye and S.-Y. Zhu, Phys. Rev. Lett. **77**, 1032 (1996).

[10] G.S. Agarwal, Phys. Rev. A**55**, 2457 (1997).

[11] P.R. Berman, Phys. Rev. A**58**, 4886 (1998).

[12] Z.G. Wang and H.R. Xia, *Molecular and Laser Spectroscopy* (Springer-Verlag, Berlin, 1991).

[13] G. Lindbad, Commun. Math. Phys. **48**, 199 (1976).

[14] S.M. Tan, J. Opt. B **1**, 424 (1999).

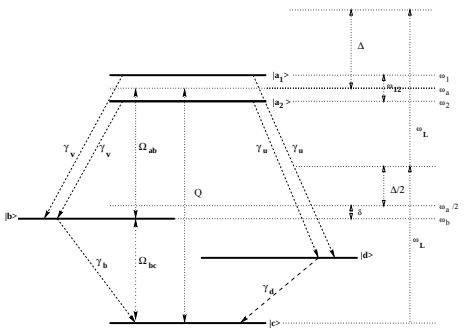

FIG. 1. Energy level structure and couplings of the molecular system.

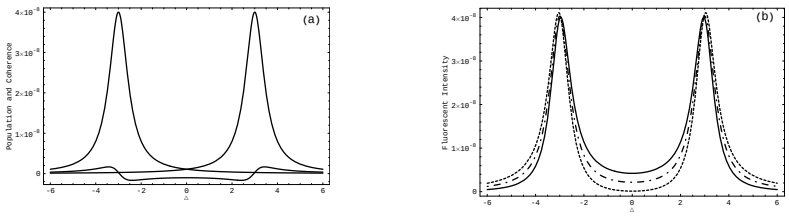

FIG. 2. Analytical results for 2-photon coupling only. (a) shows populations (ρ_{11} peaked to the left, ρ_{22} peaked to the right) and coherence ($\Re\rho_{12}$, below the axis) of the excited states. (b) shows the total fluorescent intensity in units of the spontaneous emission rate. The solid line shows the intensity on the ultraviolet transition ($p_u = -1$), the dashed line the intensity on the visible transition ($p_v = 1$), and the dash-dot line the hypothetical intensity for a transition with orthogonal dipole moments ($p = 0$). The parameters are $\Omega_{ab} = \Omega_{bc} = 0, Q = 10^{-4}, \omega_{12} = 6, \delta = 0, \gamma_u = \gamma_v = 0.5, \gamma_b = 1$. The two-photon detuning Δ is plotted in units of $\gamma_u + \gamma_v$.

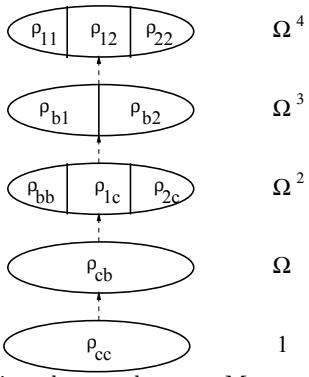

FIG. 3. Diagram showing the method for solving the steady state Master equation under the weak field assumption. The symbols on the right represent the order of the matrix elements.

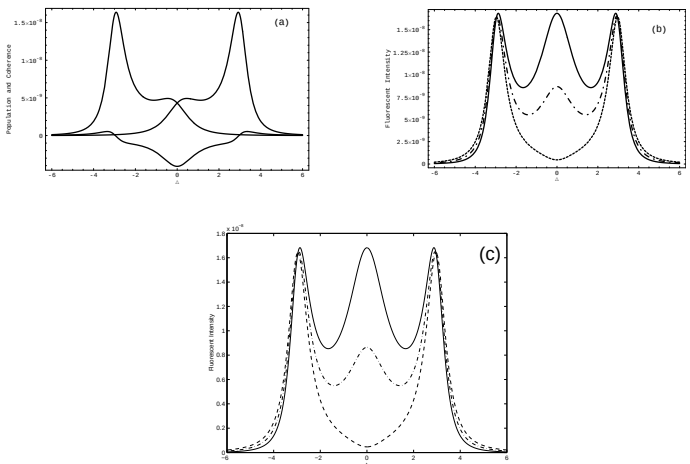

FIG. 4. Weak field results for one- and two-photon driving. (a) shows analytical populations and coherences of the the excited states, as in Fig. 2(a). (b) shows the analytical results and (c) the numerical results for the total fluorescent intensity in units of the spontaneous emission rate. The different line styles are as in Fig. 2(b). The parameters are $\Omega_{ab} = \Omega_{bc} = 0.01, Q = 0, \omega_{12} = 6, \delta = 0, \gamma_u = \gamma_v = 0.5, \gamma_b = 1$. The two-photon detuning Δ is plotted in units of $\gamma_u + \gamma_v$.

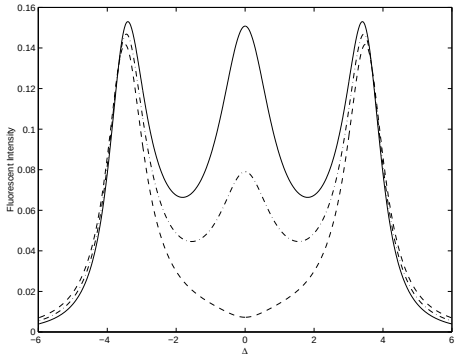

FIG. 5. Total fluorescent intensity in units of the spontaneous emission rate for strong one- and two-photon coupling. The different line styles are as in Fig. 2(b). The parameters are $\Omega_{ab} = \Omega_{bc} = 1, Q = 0, \omega_{12} = 6, \delta = 0, \gamma_u = \gamma_v = 0.5, \gamma_b = 0.15$. The two-photon detuning Δ is plotted in units of $\gamma_u + \gamma_v$.

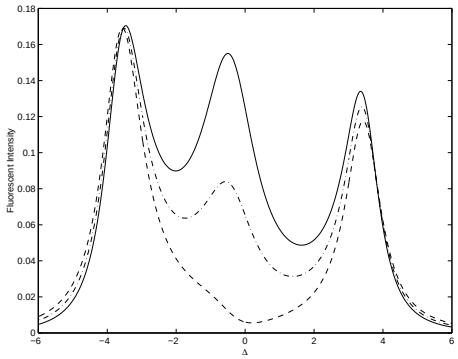

FIG. 6. Total fluorescent intensity in units of the spontaneous emission rate for strong one- and two-photon coupling, with non-zero detuning δ of the intermediate level $|b\rangle$. The different line styles are as in Fig. 2(b). The parameters are $\Omega_{ab} = \Omega_{bc} = 1, Q = 0, \omega_{12} = 6, \delta = 0.3, \gamma_u = \gamma_v = 0.5, \gamma_b = 0.15$. The two-photon detuning Δ is plotted in units of $\gamma_u + \gamma_v$.

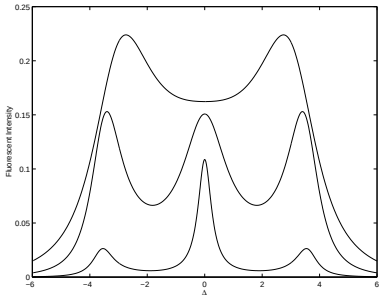

FIG. 7. Total fluorescent intensity in units of the spontaneous emission rate for strong one- and two-photon coupling. Only the ultraviolet ($p_u = -1$) transition is plotted, but $\gamma_b = \alpha\gamma_u$ is varied. The values of α for the three curves are, from top to bottom, 2, 0.3, and 0.02. The other parameters are $\Omega_{ab} = \Omega_{bc} = 1, Q = 0, \omega_{12} = 6, \delta = 0, \gamma_u = \gamma_v = 0.5$. The two-photon detuning Δ is plotted in units of $\gamma_u + \gamma_v$.

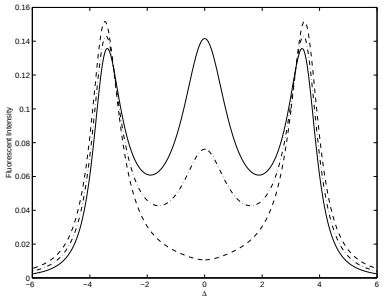

FIG. 8. Total fluorescent intensity in units of the spontaneous emission rate for strong one- and two-photon coupling, with non-equal decay rates on the ultraviolet and visibile transitions. The different line styles are as in Fig. 2(b). The parameters are $\Omega_{ab} = \Omega_{bc} = 1, Q = 0, \omega_{12} = 6, \delta = 0, \gamma_u = 0.7, \gamma_v = 0.3, \gamma_b = 0.15$. The two-photon detuning Δ is plotted in units of $\gamma_u + \gamma_v$.